Received February 1998
Revised January 1999
Accepted February 1999

A hybrid finite element-finite difference method for thermal analysis in X-ray lithography

W. Dai and R. Nassar
College of Engineering and Science, Louisiana Tech University, Ruston, Louisiana, USA

Keywords *Finite element, Finite difference, Multilayers, Thermal analysis*

Abstract *X-ray lithography is an important technique in micro fabrication used to obtain structures and devices with a high aspect ratio. The X-ray exposure takes place in a system composed of a mask and a photoresist deposited on a substrate (with a gap between mask and resist). Predictions of the temperature distribution in three dimensions in the different layers (mask, gap, photoresist and substrate) and of the potential temperature rise are essential for determining the effect of high flux X-ray exposure on distortions in the photoresist due to thermal expansion. In this study, we develop a three-dimensional numerical method for obtaining the temperature profile in an X-ray irradiation process by using a hybrid finite element-finite difference scheme for solving three-dimensional parabolic equations on thin layers. A domain decomposition algorithm is then obtained based on a parallel Gaussian elimination for solving block tridiagonal linear systems. The method is illustrated by a numerical method.*

Nomenclature

$\mathbf{A}, \mathbf{B}, D, \mathbf{D}, K, \mathbf{K}, U, \mathbf{D_1}$	= matrix	x, y, z	= coordinates
c_p	= specific heat	$\vec{\mathbf{x}}$	= eigenvector
H_1, H_2, H_3, H_4	= thickness		
h_c	= convective heat transfer coefficient	*Greek symbols*	
		$\alpha, \alpha_1, \alpha_2, \alpha_3, \alpha_4$	= thermal diffusivity
g, g_1, g_2, g_3, g_4	= source term	Δt	= time increment
k_1, k_2, k_3, k_4	= thermal conductivity	Δz	= grid size in the z-direction
N, N_z	= number of grid points	μ	= absorption coefficient
n	= the nth time step	ρ	= density
		λ, ξ, σ	= eigenvalue
r	= radius	φ_p	= basic function
r_1, r_2, r_3, r_4	= mesh ratio	ω	= relaxation parameter
T, T_1, T_2, T_3, T_4	= temperature		
T_h	= test function		
T_∞	= surrounding temperature	*Subscripts*	
		i	= layer
t	= time	m	= grid point in the z-direction
W_o	= irradiance		

International Journal of Numerical Methods for Heat & Fluid Flow, Vol. 9 No. 6, 1999, pp. 660-676.

This research is supported by a Louisiana Educational Quality Support Fund (LEQSF) grant. Contract No: LEQSF (1996-98)-RD-A-21.

1. Introduction

X-ray lithography is an important technique in micro fabrication used to obtain structures and devices with a high aspect ratio. The X-ray exposure takes place in a system composed of a mask and a photoresist, such as polymethylmethacrylate (PMMA), deposited on a substrate, as shown in Figure 1. The mask layer creates a desired pattern on the photoresist by selectively allowing the transmission of irradiation from an X-ray beam. After exposure, the photoresist is developed to remove the irradiated area, leaving behind an imprint of the pattern in the form of exposed substrate and photoresist walls. The pattern can now be used as a micromold. Electroplating can then be used to fill the mold with a metal. The remaining unexposed part of the photoresist can then be removed by an etchant, leaving the free standing microstructure on the substrate.

For rapid manufacturing of microdevices needed for commercialization, exposure times in minutes from high flux synchrotron sources may be needed. However, with the higher flux, heating of the photoresist may develop. Hence, the study of thermal effects, such as temperature rise and temperature distribution, induced in resist during X-ray exposure is important for the optimization of exposure condition (Manohara *et al.*, 1996). Analytic solutions (such as using the Green's function method (Cozisik, 1980)) to the system of these differential equations describing heat flow in the process are not easy to obtain due to the complication of the three-dimensional case and the fact that the value at the interfacial boundary between layers is unknown. Only a few

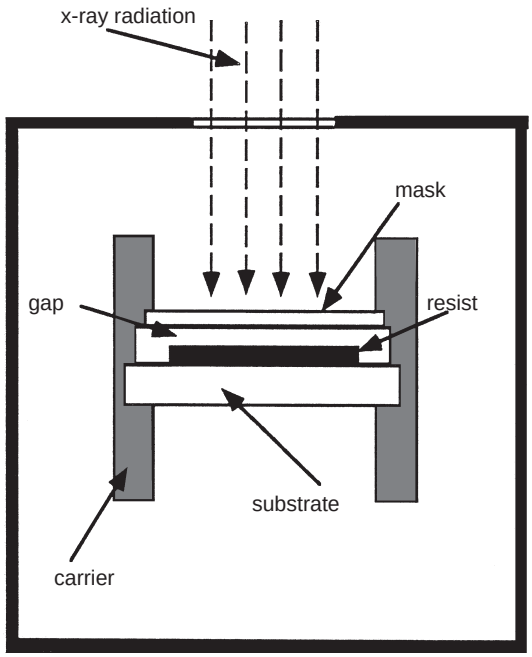

Figure 1.
Schematic diagram of an X-ray lithography system

studies have considered these kind of problems in the literature (Ameel *et al.*, 1994; Cole and McGahan, 1993; Feiertag *et al.*, 1997; Madison and McDaniel, 1989). Kant (1988, pp. 93-7) considered a laser absorption geometry that was limited to either a single interface or multiple interfaces between layers. The transient heat transfer equation was solved using the Laplace transform appropriate for the temperature rise caused by a single pulse. Madison and McDaniel (1989) also considered transient pulses of a scanned laser beam with arbitrary absorption across the source layer. Globally defined Green's functions and Laplace transforms were used to obtain solutions for temperature profiles resulting from the absorption of normally incident continuous and pulsed-Gaussian-beam irradiation. Cole and McGahan (1993) presented a method for temperature prediction in anisotropic multilayer materials that includes contact resistance between the layers for axisymmetric chopped-beam laser heating. Their method was based on a local Green's function for each layer. Ameel *et al.* (1994) developed simplified one- and two-dimensional analytical solutions and an FEM model to the problem of X-ray heating of multilayers for both uniform absorption and for absorption that decreases exponentially with depth. Feiertag *et al.* (1997) and Li *et al.* (1996) used a finite element analysis in three dimensions to study the thermoelastic mask deformation in deep X-ray lithography with synchrotron radiation. Recently, Dai *et al.* (1997) and Dai and Nassar (1997) have developed several numerical heat transfer models for thermal analysis in X-ray irradiated photoresists. The steady state temperature distribution in the resist has been obtained by solving the unsteady state differential equations in the case of two layers, resist and substrate, with a rectangular or cylindrical geometry. The authors further developed preconditioned Richardson methods to investigate the steady state temperature distribution in an X-ray irradiation process with rectangular or cylindrical geometry, where the target consists of a mask, a resist and a substrate (with a gap between mask and resist) (Dai and Nassar, 1998a; 1998b). In Dai and Nassar (1998a; 1998b), the Poisson equation at the micro-scale was solved using a preconditioned Richardson iteration in order to obtain the steady state temperature. As we know, the usual shape of pattern on the mask is arbitrary geometry and shape of the mask is either rectangular or cylindrical geometry. Since the finite element method is an efficient method to deal with arbitrary geometry, in this study we solve three-dimensional parabolic differential equations and develop a hybrid finite element-finite difference method to investigate the transient temperature distribution in an X-ray irradiation process, where the target consists of a mask, a resist and a substrate (with a gap between mask and resist) with cylindrical geometry, as shown in Figure 2. A semi-discretized equation is first obtained by applying the finite element to the xy-cross section and the finite difference to the z-thickness direction. To solve the semi-discretized equation, the idea of the Crank-Nicolson type scheme (Canuto *et al.*, 1988) is applied so that the obtained numerical scheme is unconditionally stable. Unconditional stability is particularly important so that there are no restrictions on the mesh ratio, since the grid size in the z-direction

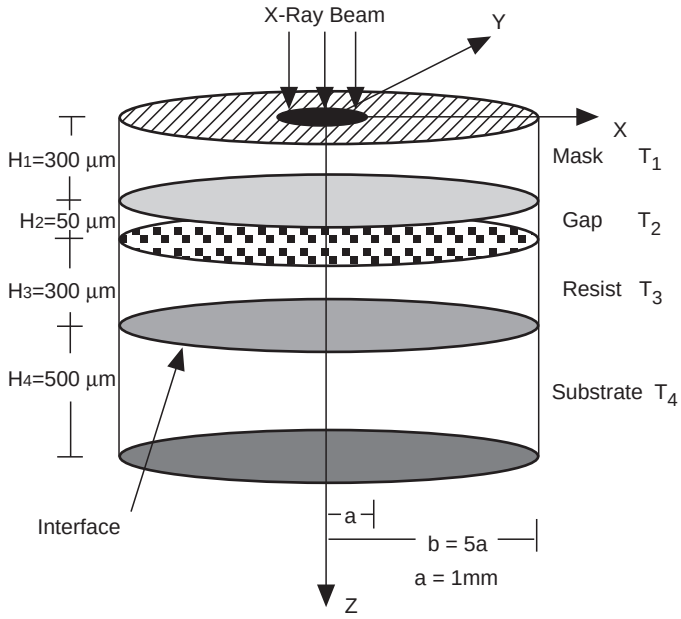

Figure 2.
Three-dimensional configuration of mask, gap, resist and substrate

is very small for simulating the X-ray lithography process. A domain decomposition algorithm is then developed for thin multilayers based on the parallel Gaussian elimination procedure for solving block tridiagonal linear systems.

2. X-ray irradiation process

We now consider an X-ray irradiation process with cylindrical geometry, where the target consists of a mask, a resist and a substrate (with a gap between mask and resist), as shown in Figure 2 (mask, resist and substrate are held in place through a special clamping mechanism not shown in the figure). A gap exists between mask and resist which contains a gas such as He. The resist such as PMMA is bonded and can be on a substrate, such as silicon. Without loss of generality, we consider that the cylindrical mask, resist and substrate are very thin, of the order of 300μm, 300 μm and 500 μm respectively, with a radius of 5 mm. The gap is also very thin, of the order of 50μm. To study the effect of the high flux X-ray exposure on distortions in the resist, it is important to predict the temperature distribution in the resist and the substrate. Much of the incident radiation is transmitted through the mask. Only the absorbed energy is transmitted by conduction. Due to the very thin gap and the relatively low temperature, radiation can be neglected. Also, the cooling effect resulting from free convection is negligible and therefore heat is mainly transferred by conduction through the gap (Li *et al.*, 1996). Heat is then transferred by conduction through the resist and substrate. We assume that the resist layer is on a thick substrate which is well cooled and remains at a fixed temperature

(Ameel *et al.*, 1994). Following the procedure in Ameel *et al.* (1994), we express the governing equations for heat conduction as follows:

Mask

$$\frac{\partial T_1}{\partial t} = \alpha_1 \left(\frac{\partial^2 T_1}{\partial x^2} + \frac{\partial^2 T_1}{\partial y^2} + \frac{\partial^2 T_1}{\partial z^2} \right) + g_1(x, y, z, t); \tag{1}$$

Gap

$$\frac{\partial T_2}{\partial t} = \alpha_2 \left(\frac{\partial^2 T_2}{\partial x^2} + \frac{\partial^2 T_2}{\partial y^2} + \frac{\partial^2 T_2}{\partial z^2} \right) + g_2(x, y, z, t); \tag{2}$$

Resist

$$\frac{\partial T_3}{\partial t} = \alpha_3 \left(\frac{\partial^2 T_3}{\partial x^2} + \frac{\partial^2 T_3}{\partial y^2} + \frac{\partial^2 T_3}{\partial z^2} \right) + g_3(x, y, z, t); \tag{3}$$

Substrate

$$\frac{\partial T_4}{\partial t} = \alpha_4 \left(\frac{\partial^2 T_4}{\partial x^2} + \frac{\partial^2 T_4}{\partial y^2} + \frac{\partial^2 T_4}{\partial z^2} \right) + g_4(x, y, z, t); \tag{4}$$

where $T_1, T_2, T_3, T_4, \alpha_1, \alpha_2, \alpha_3, \alpha_4$ are temperatures, and thermal diffusivities respectively. The source term $g_i(x, y, z, t)(i = 1, 2, 3, 4)$ depends on the mode of the system and can be determined by experiments. The boundary conditions are described as follows:

On the top surface of the mask, $z = 0$, where heat convection occurs,

$$k_1 \frac{\partial T_1}{\partial z} = h_c (T_1 - T_\infty), \tag{5}$$

where T_∞ is the temperature of the surroundings and h_c is the convection coefficient.

On the bottom surface of the mask, $z = H_1$, we assume that the flux across the interface does not change,

$$-k_1 \frac{\partial T_1}{\partial z} = -k_2 \frac{\partial T_2}{\partial z}, \qquad \text{and} \quad T_1 = T_2. \tag{6}$$

Similarly, on the top surface of the resist, $z = H_1 + H_2$,

$$-k_2 \frac{\partial T_2}{\partial z} = -k_3 \frac{\partial T_3}{\partial z}, \qquad \text{and} \quad T_3 = T_2. \tag{7}$$

On the bottom surface of the resist, $z = H_1 + H_2 + H_3$,

$$-k_3 \frac{\partial T_3}{\partial z} = -k_4 \frac{\partial T_4}{\partial z}, \quad T_3 = T_4. \tag{8}$$

Under experimental conditions, the side walls of the mask, resist and substrate (Figure 2), and the bottom surface of the substrate are maintained at a nearly uniform temperature as a result of its contact with a heat sink that is designed to promote heat dissipation. As such, it is realistic to assume $T_i = T_\infty,\ i = 1,2,3,4$, on the side walls, and $T_4 = T_\infty$ on the bottom surface of the substrate.

3. Numerical model

The numerical model is developed based on a hybrid finite element-finite difference scheme, and the idea of Crank-Nicolson type scheme for parabolic differential equations. A domain decomposition algorithm is then obtained based on a parallel Gaussian elimination technique for solving block tridiagonal linear systems. To this end, we first apply the finite element method for the *xy*-cross section.

3.1. Semi-discretized equation

We consider a three-dimensional parabolic differential equation in a cylindrical domain, as shown in Figure 2,

$$\frac{\partial T}{\partial t} = \alpha\left(\frac{\partial^2 T}{\partial x^2} + \frac{\partial^2 T}{\partial y^2} + \frac{\partial^2 T}{\partial z^2}\right) + g(x,y,z,t), \tag{9}$$

where α is thermal diffusivity. We assume that $T = 0$ when the point (x,y,z) is at the side wall. Let

$$\begin{aligned} &\iint_G \left\{\frac{\partial T}{\partial t}v - \mu\left(\frac{\partial^2 T}{\partial x^2} + \frac{\partial^2 T}{\partial y^2} + \frac{\partial^2 T}{\partial z^2}\right)v - gv\right\}dxdy \\ &= \iint_G \left\{\frac{\partial T}{\partial t}v + \mu\left(\frac{\partial T}{\partial x}\frac{\partial v}{\partial x} + \frac{\partial T}{\partial y}\frac{\partial v}{\partial y}\right) - \mu\frac{\partial^2 T}{\partial z^2}v - gv\right\}dxdy \\ &= 0, \end{aligned} \tag{10}$$

where $v(x,y)$ is a function in the Sobolev space H_o^1 (Carey and Oden, 1984). Without loss of generality, we consider that a finite element mesh is constructed in the *xy*-cross section (as shown in Figure 3). A test function for $T(x,y,z,t)$ is then chosen to be

$$T_h(x,y,z,t) = \sum_{p=1}^{N} T_p(z,t)\varphi_p(x,y), \tag{11}$$

where $\varphi_p(x,y)$ is a basic function (e.g. linear basic function), N is the number of grid points in the *xy*-cross section. Also, we consider $g_h(x,y,z,t) = \sum_{p=1}^{N} g_p(z,t)\varphi_p(x,y)$ as an interpolant of $g(x,y,z,t)$. Substituting $T_h(x,y,z,t)$ and $g_h(x,y,z,t)$ into (10), we obtain

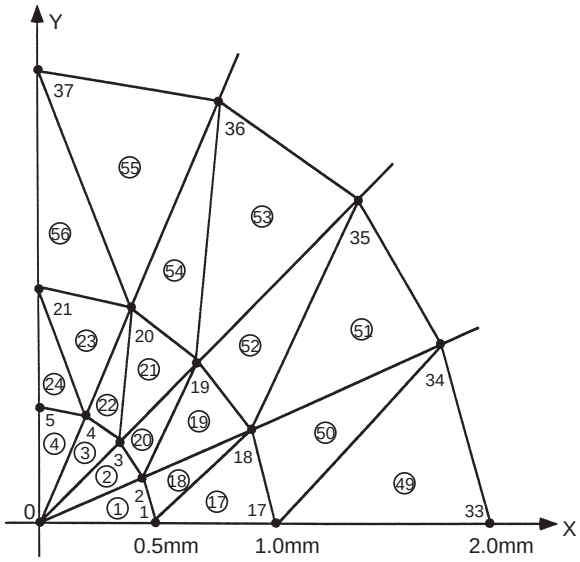

Figure 3.
Part of the finite element mesh in the *xy* cross section

$$\sum_{p=1}^{N}\frac{\partial T_p}{\partial t}\iint_G \varphi_p v dxdy$$
$$+\sum_{p=1}^{N}\left\{\alpha T_p\iint_G\left(\frac{\partial\varphi_p}{\partial x}\frac{\partial v}{\partial x}+\frac{\partial\varphi_p}{\partial y}\frac{\partial v}{\partial y}\right)dxdy-\alpha\frac{\partial^2 T_p}{\partial z^2}\iint_G\varphi_p v dxdy\right\} \quad (12)$$
$$-\sum_{p=1}^{N}g_p\iint_G\varphi_p v dxdy=0.$$

If we choose $v=\varphi_q$, then (12) becomes

$$\sum_{p=1}^{N}\frac{\partial T_p}{\partial t}\iint_G \varphi_p\varphi_q dxdy$$
$$+\sum_{p=1}^{N}\left\{\alpha T_p\iint_G\left(\frac{\partial\varphi_p}{\partial x}\frac{\partial\varphi_q}{\partial x}+\frac{\partial\varphi_p}{\partial y}\frac{\partial\varphi_q}{\partial y}\right)dxdy-\alpha\frac{\partial^2 T_p}{\partial z^2}\iint_G\varphi_p\varphi_q dxdy\right\} \quad (13)$$
$$-\sum_{p=1}^{N}g_p\iint_G\varphi_p\varphi_q dxdy=0,\qquad q=1,2,\cdots,N.$$

Introducing the vector notations $\vec{T}(z,t)=(T_1(z,t),\cdots,T_N(z,t))^T$, $\vec{f}(z,t)=(g_1,\cdots,g_N)^T$ and the matrices M_{NxN} and K_{NxN} with the two respective entries,

$$m_{qp}=\iint_G\varphi_p\varphi_q dxdy\quad\text{and}\quad k_{qp}=\iint_G\left(\frac{\partial\varphi_p}{\partial x}\frac{\partial\varphi_q}{\partial x}+\frac{\partial\varphi_p}{\partial y}\frac{\partial\varphi_q}{\partial y}\right)dxdy, \quad (14)$$

we can express system (13) in matrix form as follows:

$$M\frac{\partial \vec{T}}{\partial t}+\alpha K\vec{T}-\alpha M\frac{\partial^2 \vec{T}}{\partial z^2}=M\vec{f}. \tag{15}$$

For simplification, we apply the lumped mass technique (Carey and Oden, 1984; Chandrupatla and Belegundu, 1991) to obtain a diagonal matrix D and then replace M by D in (15) to give

$$D\frac{\partial \vec{T}}{\partial t}+\alpha K\vec{T}-\alpha D\frac{\partial^2 \vec{T}}{\partial z^2}=D\vec{f}, \tag{16}$$

where each entry d_p at the diagonal of D is $\frac{1}{3}\sum_{\Delta} S_{\Delta}$ (i.e. one-third of the sum of all elements with node p as one vertex).

Let $\vec{T}_m=\vec{T}(m\Delta z,t)$, where Δz is the grid size in the z-direction, $m=1,\cdots,N_z$. Using a second-order standard finite difference to approximate $\frac{\partial^2 \vec{T}}{\partial z^2}$, we obtain a semi-discretized equation for (16) as follows:

$$D\frac{\partial \vec{T}_m}{\partial t}+\alpha K\vec{T}_m-\frac{\alpha}{\Delta z^2}D\left(\vec{T}_{m+1}-2\vec{T}_m+\vec{T}_{m-1}\right)=D\vec{f}_m,\quad m=1,\cdots,N_z, \tag{17}$$

It should be pointed out that K and D are symmetric and positive definite, and the entries of K satisfy $k_{pp}\geq\sum_{\substack{q=1\\ p\neq q}}^{N}|k_{pq}|, p=1,\cdots,N$.

3.2. Crank-Nicolson type scheme

The simplest practical time discretization of (17) is the Crank-Nicolson type scheme (Canuto *et al.*, 1988). Since K is a sparse matrix, we define a diagonal matrix D_1 with a diagonal entry, $d_p=2k_{pp}$, where k_{pp} is the entry on the main diagonal line of the matrix K, and $p=1,2,\cdots,N$. Thus, based on the idea of the Crank-Nicolson type scheme, a numerical scheme can be obtained as follows:

$$\begin{aligned}D\frac{\vec{T}_m^{n+1}-\vec{T}_m^{n}}{\Delta t}+\frac{\alpha}{2}D_1\vec{T}_m^{n+1}-\frac{\alpha}{2\Delta z^2}D\left(\vec{T}_{m+1}^{n+1}-2\vec{T}_m^{n+1}+\vec{T}_{m-1}^{n+1}\right)\\ =\frac{\alpha}{2}D_1\vec{T}_m^{n}-\alpha K\vec{T}_m^{n}+\frac{\alpha}{2\Delta z^2}D\left(\vec{T}_{m+1}^{n}-2\vec{T}_m^{n}+\vec{T}_{m-1}^{n}\right)\\ +D\vec{f}_m^{n+1/2}\end{aligned} \tag{18}$$

$$m=1,\cdots,N_z,\ n=0,1,2,\cdots,$$

where $\vec{T}_m^{n}=\vec{T}(m\Delta z,n\Delta t)$, $\vec{f}_m^{n+1/2}=\vec{f}(m\Delta z,(n+\frac{1}{2})\Delta t)$, Δt is the time increment, and $n\Delta t\leq t_o$. It can be seen that the above scheme (18) is first-order accurate in Δt.

To discuss the stability of (18), we introduce the following notations for matrices and vectors,

$$\mathbf{K}=\begin{bmatrix} K & & \\ & \ddots & \\ & & K \end{bmatrix}, \mathbf{D}=\begin{bmatrix} D & & \\ & \ddots & \\ & & D \end{bmatrix}, \mathbf{D_1}=\begin{bmatrix} D_1 & & \\ & \ddots & \\ & & D_1 \end{bmatrix},$$

$$\mathbf{U}=\begin{bmatrix} 2D & -D & & & \\ -D & 2D & -D & & \\ & & \ddots & & \\ & & -D & 2D & -D \\ & & & -D & 2D \end{bmatrix}, \vec{\mathbf{G}}^{n+1/2}=\begin{bmatrix} \vec{f}_1^{1/2} \\ \vdots \\ \vec{f}_{Nz}^{n+1/2} \end{bmatrix}, \vec{\mathbf{T}}^{n}=\begin{bmatrix} \vec{T}_1^{n} \\ \vdots \\ \vec{T}_{Nz}^{n} \end{bmatrix}.$$

Thus, we can rewrite (18) into a matrix form as follows:

$$\begin{aligned}\left(\frac{1}{\Delta t}\mathbf{D}+\frac{\alpha}{2}\mathbf{D_1}+\frac{\alpha}{2\Delta z^2}\mathbf{U}\right)\vec{T}^{n+1}=&\left(\frac{1}{\Delta t}\mathbf{D}+\frac{\alpha}{2}\mathbf{D_1}+\frac{\alpha}{2\Delta z^2}\mathbf{U}\right)\vec{\mathbf{T}}^{\mathbf{n}}\\ &-\left[(\alpha\mathbf{K}+\frac{\alpha}{\Delta z^2}\mathbf{U})\vec{\mathbf{T}}^{\mathbf{n}}-\mathbf{D}\vec{\mathbf{G}}^{n+1/2}\right].\end{aligned} \tag{19}$$

Let $\mathbf{A}=\frac{1}{\Delta t}\mathbf{D}+\frac{\alpha}{2}\mathbf{D_1}+\frac{\alpha}{2\Delta z^2}\mathbf{U}$ and $\mathbf{B}=\mathbf{I}-\mathbf{A}^{-1}\left(\alpha\mathbf{K}+\frac{\alpha}{\Delta z^2}\mathbf{U}\right)$. Then (19) becomes

$$\vec{\mathbf{T}}^{\mathbf{n+1}}=\mathbf{B}\vec{\mathbf{T}}^{\mathbf{n}}+\mathbf{A}^{-\mathbf{1}}\mathbf{D}\vec{\mathbf{G}}^{n+1/2.} \tag{20}$$

To determine the stability of (20), it is necessary to compute the eigenvalues of the amplification matrix $\mathbf{B}$. Based on the theory given in Atkinson (1988), the quantity $\mathbf{B}^l\vec{\mathbf{T}}^n \to \vec{0}$ as $l \to \infty$ for any $\vec{\mathbf{T}}^n \in R^{NzN}$ if the eigenvalue λ of $\mathbf{B}$ satisfies $|\lambda|<1$. Let ξ be an eigenvalue of $\mathbf{A}^{-1}\left(\alpha\mathbf{K}+\frac{\alpha}{\Delta z^2}\mathbf{U}\right)$ and $\vec{\mathbf{x}}$ be an eigenvector corresponding to ξ such that

$$\left(\alpha\mathbf{K}+\frac{\alpha}{\Delta z^2}\mathbf{U}\right)\vec{\mathbf{x}}=\xi\left(\frac{1}{\Delta t}\mathbf{D}+\frac{\alpha}{2}\mathbf{D_1}+\frac{\alpha}{2\Delta z^2}\mathbf{U}\right)\vec{\mathbf{x}}. \tag{21}$$

Thus, the eigenvalue λ of $\mathbf{B}$ is

$$\lambda=1-\xi. \tag{22}$$

Since K and D are symmetric and positive definite, $\mathbf{D}, \mathbf{D}_1$, and $\mathbf{K}$ are symmetric and positive definite. Also, it can be seen that $\mathbf{U}$ is symmetric and positive definite. Thus, ξ is positive and can be obtained as follows:

$$\xi=\frac{\alpha\vec{\mathbf{x}}^{\mathbf{T}}\mathbf{K}\vec{\mathbf{x}}+\frac{\alpha}{\Delta z^2}\vec{\mathbf{x}}^{\mathbf{T}}\mathbf{U}\vec{\mathbf{x}}}{\frac{1}{\Delta t}\vec{\mathbf{x}}^{\mathbf{T}}\mathbf{D}\vec{\mathbf{x}}+\frac{\alpha}{2}\vec{\mathbf{x}}^{\mathbf{T}}\mathbf{D_1}\vec{\mathbf{x}}+\frac{\alpha}{2\Delta z^2}\vec{\mathbf{x}}^{\mathbf{T}}\mathbf{U}\vec{\mathbf{x}}}. \tag{23}$$

Theorem. The eigenvalue λ of $\mathbf{B}$ satisfies $|\lambda|<1$. Hence, scheme (20) is unconditionally stable.

Proof. It can be seen that $\vec{\mathbf{x}}^{\mathbf{T}}\mathbf{K}\vec{\mathbf{x}} \le \vec{\mathbf{x}}^{\mathbf{T}}\mathbf{D_1}\vec{\mathbf{x}}$. In fact, from the entry $k_{pp} \ge \sum_{\substack{p=1 \\ p\neq q}}^{N} |k_{pq}|$, we obtain by the Gerschgorin theorem [3] that the eigenvalue σ_p of K satisfies $|\sigma_p - k_{pp}| \le \sum_{\substack{q=1 \\ p\neq q}}^{N} |k_{pq}| \le k_{pp}$. Therefore, $2k_{pp} - \sigma_p \ge 0$. Since D_1 is a diagonal matrix with a diagonal entry, $d_p = 2k_{pp}$, we obtain from linear algebra (Anton, 1994) that $D_1 - K$ and hence $\mathbf{D_1} - \mathbf{K}$ are symmetric and positive semi-definite. This results in $\vec{\mathbf{x}}^{\mathbf{T}}\mathbf{K}\vec{\mathbf{x}} \le \vec{\mathbf{x}}^{\mathbf{T}}\mathbf{D_1}\vec{\mathbf{x}}$. Hence, we obtain from (23) that $0 < \xi < 2$. We conclude that $|\lambda| = |1 - \xi| < 1$.

3.3. Domain decomposition algorithm

We now apply scheme (18) to solve (1)-(8) and write the scheme as follows:

$$\begin{aligned} D\frac{(\vec{T}_i)_m^{n+1} - (\vec{T}_i)_m^n}{\Delta t} + \frac{\alpha_i}{2}D_1\left(\vec{T}_i\right)_m^{n+1} - \frac{\alpha_i}{2\Delta z_i^2}D\Bigg(\left(\vec{T}_i\right)_{m+1}^{n+1} \\ - 2\left(\vec{T}_i\right)_m^{n+1} + \left(\vec{T}_i\right)_{m-1}^{n+1}\Bigg) \\ = \frac{\alpha_i}{2}D_1\left(\vec{T}_i\right)_m^{n} - \alpha_i K\left(\vec{T}_i\right)_m^{n} \\ + \frac{\alpha_i}{2\Delta z_i^2}D\Bigg(\left(\vec{T}_i\right)_{m+1}^{n} - 2\left(\vec{T}_i\right)_m^{n} + \left(\vec{T}_i\right)_{m-1}^{n}\Bigg) \\ + D\left(\vec{g}_i\right)_m^{n+1/2}, \quad m = 1, \cdots, N_z^{(i)},\ n = 0, 1, 2, \cdots, \end{aligned} \tag{24}$$

where $i = 1, 2, 3, 4$. At each time step, $(\vec{T}_i)_m^{n+1}$ is assumed to satisfy the discrete boundary and interfacial conditions as follows:

$$k_1\frac{\left(\vec{T}_1\right)_1^{n+1} - \left(\vec{T}_1\right)_0^{n+1}}{\Delta z_1} = h_c\left(\left(\vec{T}_1\right)_0^{n+1} - \vec{T}_\infty\right), \quad z = 0, \tag{25a}$$

$$\begin{cases} -k_1\dfrac{\left(\vec{T}_1\right)_{N_z^{(1)}+1}^{n+1} - \left(\vec{T}_1\right)_{N_z^{(1)}}^{n+1}}{\Delta z_1} = -k_2\dfrac{\left(\vec{T}_2\right)_1^{n+1} - \left(\vec{T}_2\right)_0^{n+1}}{\Delta z_2}, \\ \left(\vec{T}_1\right)_{N_z^{(1)}+1}^{n+1} = \left(\vec{T}_2\right)_0^{n+1}, \end{cases} \quad z = H_1, \tag{25b}$$

$$\begin{cases} -k_2 \dfrac{\left(\vec{T}_2\right)_{N_z^{(2)}+1}^{n+1} - \left(\vec{T}_2\right)_{N_z^{(2)}}^{n+1}}{\Delta z_2} = -k_3 \dfrac{\left(\vec{T}_3\right)_1^{n+1} - \left(\vec{T}_3\right)_0^{n+1}}{\Delta z_3}, \\ \left(\vec{T}_2\right)_{N_z^{(2)}+1}^{n+1} = \left(\vec{T}_3\right)_0^{n+1}, \end{cases} \quad z = H_1 + H_2, \quad (25c)$$

$$\begin{cases} -k_3 \dfrac{\left(\vec{T}_3\right)_{N_z^{(3)}+1}^{n+1} - \left(\vec{T}_3\right)_{N_z^{(3)}}^{n+1}}{\Delta z_3} = -k_4 \dfrac{\left(\vec{T}_4\right)_1^{n+1} - \left(\vec{T}_4\right)_0^{n+1}}{\Delta z_4}, \\ \left(\vec{T}_3\right)_{N_z^{(3)}+1}^{n+1} = \left(\vec{T}_4\right)_0^{n+1}, \end{cases} \quad z = H_1 + H_2 + H_3, \quad (25d)$$

On the other boundaries,

$$\left(\vec{T}_i\right)_m^{(n+1)} = T_\infty, \quad (i = 1, 2, 3, 4). \quad (26)$$

$\left\{(\vec{T}_i)_m^{(n+1)}\right\}(i = 1, 2, 3, 4)$ are computed by equation (24). As such, we express these equations as four block tridiagonal linear systems.

$$-r_i D\left(\vec{T}_i\right)_{m-1}^{n+1} + ((2r_i + 1)D + a_i D_1)\left(\vec{T}_i\right)_m^{n+1} - r_i D\left(\vec{T}_i\right)_{m+1}^{n+1} = \left(\vec{f}_i\right)_m^n, \quad m = 1, \cdots, N_z^i \quad (27)$$

where $r_i = \frac{\alpha_i \Delta t}{2\Delta z_i^2}$ and $a_i = \frac{\alpha_i \Delta t}{2}, i = 1, 2, 3, 4$. Since $\left\{(\vec{T}_i)_m^{n+1}\right\}(i = 1, 2, 3, 4)$ are unknown at the interface between layers, the above four block tridiagonal linear systems cannot be solved. To overcome this difficulty, we apply a parallel Gaussian elimination (as described in Dai and Nassar (1998)) for solving block tridiagonal linear systems. As such, a domain decomposition algorithm for thermal analysis in the X-ray irradiation process can be described as follows:

Step 1. Calculate the coefficient sequences $\left\{A_m^{(1)}, \mathbf{v}_m^{(1)}\right\}$, $\left\{A_m^{(2)}, \mathbf{v}_m^{(2)}, \mathbf{w}_m^{(2)}\right\}$, $\left\{\tilde{A}_m^{(2)}, \tilde{\mathbf{v}}_m^{(2)}, \tilde{\mathbf{w}}_m^{(2)}\right\}$, $\left\{A_m^{(3)}, \mathbf{v}_m^{(3)}, \mathbf{w}_m^{(3)}\right\}$, $\left\{\tilde{A}_m^{(3)}, \tilde{\mathbf{v}}_m^{(3)}, \tilde{\mathbf{w}}_m^{(3)}\right\}$, and $\left\{\tilde{A}_m^{(4)}, \tilde{\mathbf{v}}_m^{(4)}\right\}$ as follows:

$$A_m^{(1)} = \left[(2r_1 + 1)D + a_1 D_1 - r_1 D A_{m-1}^{(1)}\right]^{-1} r_1 D, A_o^{(1)} = \mathbf{0}, \quad (28a)$$

$$\mathbf{v}_m^{(1)} = \left[(2r_1 + 1)D + a_1 D_1 - r_1 D A_{m-1}^{(1)}\right]^{-1} \left(\left(\vec{f}_1\right)_m^n + r_1 D \mathbf{v}_{m-1}^{(1)}\right), \mathbf{v}_o^{(1)} = \mathbf{0}; \quad m = 1, \cdots, N_z^{(1)}, \quad (28b)$$

$$A_m^{(i)} = \left[(2r_i + 1)D + a_i D_1 - r_i D A_{m-1}^{(i)}\right]^{-1} r_i D =, A_o^{(i)} = 0, \quad (29a)$$

$$\mathbf{v}_m^{(i)} = \left[(2r_i+1)D + a_iD_1 - r_iDA_{m-1}^{(i)}\right]^{-1}\left(\left(\vec{f}_i\right)_m^n + r_iD\mathbf{v}_{m-1}^{(i)}\right), \mathbf{v}_o^{(i)} = \mathbf{0}, \tag{29b}$$

$$\mathbf{w}_m^{(i)} = \left[(2r_i+1)D + a_iD_1 - r_iDA_{m-1}^{(i)}\right]^{-1} r_iD\mathbf{w}_{m-1}^{(i)}), \mathbf{w}_o^{(i)} = \mathbf{1}; \quad m = 1, \cdots, N_z^{(i)}, i = 2,3; \tag{29c}$$

$$\tilde{A}_m^{(i)} = \left[(2r_i+1)D + a_iD_1 - r_iD\tilde{A}_{m+1}^{(i)}\right]^{-1} r_iD, \quad \tilde{A}_{N_z^{(i)}+1}^{(i)} = 0, \tag{30a}$$

$$\tilde{\mathbf{v}}_m^{(i)} = \left[(2r_i+1)D + a_iD_1 - r_iD\tilde{A}_{m+1}^{(i)}\right]^{-1}\left(\left(\vec{f}_i\right)_m^n + r_iD\tilde{\mathbf{v}}_{m+1}^{(i)}\right), \tilde{\mathbf{v}}_{N_z^{(i)}+1}^{(i)} = \mathbf{0}, \tag{30b}$$

$$\tilde{\mathbf{w}}_m^{(i)} = \left[(2r_i+1)D + a_iD_1 - r_iD\tilde{A}_{m+1}^{(i)}\right]^{-1} r_iD\tilde{\mathbf{w}}_{m+1}^{(i)}), \tilde{\mathbf{w}}_{N_z^{(i)}+1}^{(i)} = \mathbf{1}; \quad m = N_z^{(i)}, \cdots, 1, \quad i = 2,3; \tag{30c}$$

$$\tilde{A}_m^{(4)} = \left[(2r_4+1)D + a_4D_1 - r_4D\tilde{A}_{m-1}^{(4)}\right]^{-1} r_4D, \qquad \tilde{A}_{N_z^{(4)}+1}^{(4)} = 0, \tag{31a}$$

$$\tilde{\mathbf{v}}_m^{(4)} = \left[(2r_4+1)D + a_4D_1 - r_4D\tilde{A}_{m+1}^{(4)}\right]^{-1}\left(\left(\vec{f}_4\right)_m^n + r_4D\tilde{\mathbf{v}}_{m+1}^{(4)}\right), \tilde{\mathbf{v}}_{N_z^{(4)}+1}^{(4)} = \mathbf{0}; \quad m = N_z^{(4)}, \cdots, 1. \tag{31b}$$

Step 2. Substitute the following six equations

$$\left(\vec{T}_1\right)_{N_z^{(1)}}^{n+1} = A_{N_z^{(1)}}^{(1)}\left(\vec{T}_1\right)_{N_z^{(1)}+1}^{n+1} + \mathbf{v}_{N_z^{(1)}}^{(1)},$$

$$\left(\vec{T}_2\right)_{N_z^{(2)}}^{n+1} = A_{N_z^{(2)}}^{(2)}\left(\vec{T}_2\right)_{N_z^{(2)}+1}^{n+1} + \mathbf{v}_{N_z^{(2)}}^{(2)} + \mathbf{w}_{N_z^{(2)}}^{(2)}\left(\vec{T}_2\right)_0^{n+1},$$

$$\left(\vec{T}_2\right)_1^{n+1} = \tilde{A}_1^{(2)}\left(\vec{T}_2\right)_0^{n+1} + \tilde{\mathbf{v}}_1^{(2)} + \tilde{\mathbf{w}}_1^{(2)}\left(\vec{T}_2\right)_{N_z^{(2)}+1}^{n+1},$$

$$\left(\vec{T}_3\right)_{N_z^{(3)}}^{n+1} = A_{N_z^{(3)}}^{(3)}\left(\vec{T}_3\right)_{N_z^{(3)}+1}^{n+1} + \mathbf{v}_{N_z^{(3)}}^{(3)} + \mathbf{w}_{N_z^{(3)}}^{(3)}\left(\vec{T}_3\right)_0^{n+1},$$

$$(T_3)_1^{n+1} = \tilde{A}_1^{(3)}\left(\vec{T}_3\right)_0^{n+1} + \tilde{\mathbf{v}}_1^{(3)} + \tilde{\mathbf{w}}_1^{(3)}\left(\vec{T}_3\right)_{N_z^{(3)}+1}^{n+1} \quad \text{and}$$

$$\left(\vec{T}_4\right)_1^{n+1} = \tilde{A}_1^{(4)}\left(\vec{T}_4\right)_0^{n+1} + \tilde{\mathbf{v}}_1^{(4)}$$

into the discrete boundary equations (25b)-(25d) to obtain $(\vec{T}_1)_{N_z^{(1)}+1}^{n+1}$, $(\vec{T}_2)_0^{n+1}$, $(\vec{T}_2)_{N_z^{(2)}+1}^{n+1}$, $(\vec{T}_3)_0^{n+1}$, $(\vec{T}_3)_{N_z^{(3)}+1}^{n+1}$ and $(\vec{T}_4)_0^{n+1}$.

Step 3. Solve for the rest of the unknowns in $\left\{(\vec{T}_i)_m^{n+1}\right\}(i = 1,2,3,4)$ using the following sequences:

$$\left(\vec{T}_1\right)_m^{n+1} = A_m^{(1)}\left(\vec{T}_1\right)_{m+1}^{n+1} + \psi_m^{(}1), \left(\vec{T}_1\right)_{N_z^{(1)}+1}^{n+1} = \vec{0}; \quad m = N_z^{(1)}, \cdots, 1. \tag{33a}$$

$$\left(\vec{T}_i\right)_m^{n+1} = A_m^{(i)}\left(\vec{T}_i\right)_{m+1}^{n+1} + \mathbf{v}_m^{(i)} + \mathbf{w}_m^{(i)}\left(\vec{T}_i\right)_0^{n+1}; \; m = N_z^{(i)}, \cdots, 1, \; i = 2, 3. \tag{33b}$$

$$\left(\vec{T}_4\right)_m^{n+1} = \tilde{A}_m^{(4)}\left(\vec{T}_4\right)_{m-1}^{n+1} + \tilde{\mathbf{v}}_m^{(4)}, \left(\vec{T}_4\right)_0^{n+1} = \vec{0}; \quad m = 1, \cdots, N_z^{(4)}. \tag{33c}$$

It should be pointed out that the procedures in step 1 involve many matrix inverse calculations. However, the computation is rather simple since D and D_1 are diagonal matrices. Further, this domain decomposition algorithm has a high inherent parallelism. This can be seen by the fact that equations (28)-(33) can be computed in parallel. For example, one can use five computer processes to run this algorithm. In step 1, four processes are used to calculate $\left\{A_m^{(1)}, \mathbf{v}_m^{(1)}\right\}$, $\left\{A_m^{(2)}, \mathbf{v}_m^{(2)}, \mathbf{w}_m^{(2)}\right\}$ and $\left\{\tilde{A}_m^{(2)}, \tilde{\mathbf{v}}_m^{(2)}, \tilde{\mathbf{w}}_m^{(2)}\right\}$, $\left\{A_m^{(3)}, \mathbf{v}_m^{(3)}, \mathbf{w}_m^{(3)}\right\}$ and $\left\{\tilde{A}_m^{(3)}, \tilde{\mathbf{v}}_m^{(3)}, \tilde{\mathbf{w}}_m^{(3)}\right\}$, $\left\{\tilde{A}_m^{(4)}, \tilde{\mathbf{v}}_m^{(4)}\right\}$ in parallel, and pass the information to the fifth process. Then the fifth process runs step 2 and returns the results to the first four processes. Finally, the first four processes run step 3 in parallel. This domain decomposition algorithm can be readily applied for solving three-dimensional parabolic differential equations on thin multilayers with irregular geometry in the xy-direction.

4. Numerical example

To demonstrate the applicability of the present numerical method, we investigate the maximum temperature rise within the cylindrical resist in the example given in Dai and Nassar (1998), and compare the numerical results with those obtained by using a preconditioned Richardson iteration for solving the corresponding elliptic equations, which was developed in Dai and Nassar (1998). The preconditioned Richardson iteration corresponding to scheme (24) can be written as follows:

$$\begin{aligned}
&\alpha_i D_1\left(\vec{T}_i\right)_m^{(n+1)} - \frac{\alpha_i}{\Delta z_i^2} D\left(\left(\vec{T}_i\right)_{m+1}^{(n+1)} - 2\left(\vec{T}_i\right)_m^{(n+1)} + \left(\vec{T}_i\right)_{m-1}^{(n+1)}\right) \\
&\qquad = \alpha_i D_1\left(\vec{T}_i\right)_m^{(n)} - \frac{\alpha_i}{\Delta z_i^2} D\left(\left(\vec{T}_i\right)_{m+1}^{(n)} - 2\left(\vec{T}_i\right)_m^{(n)} + \left(\vec{T}_i\right)_{m-1}^{(n)}\right) \\
&\qquad -\omega\left[\alpha_i K\left(\vec{T}_i\right)_m^{(n)} - \frac{\alpha_i}{\Delta z_i^2} D\left(\left(\vec{T}_i\right)_{m+1}^{(n)} - 2\left(\vec{T}_i\right)_m^{(n)} + \left(\vec{T}_i\right)_{m-1}^{(n)}\right) - D\left(\vec{g}_i\right)_m\right] \\
&\qquad m = 1, \cdots, N_z^{(i)}, \; n = 0, 1, 2, \cdots, \quad i = 1, 2, 3, 4,
\end{aligned} \tag{34}$$

where $0 \leq \omega \leq 1$ is a relaxation parameter and n is an iteration number.

We apply both the present method and the preconditioned Richardson method to an X-ray irradiation process, where the target consists of a mask, a resist and a substrate (with a gap between mask and resist), as shown in Figure 2. In this example, beryllium, He gas, PMMA and silicon were used for the mask, gap, resist and substrate respectively. The heat absorption in each layer is the exponential expression (Ameel *et al.*, 1994):

$$g_i(x,y,z,t) = \begin{cases} (W_o)_i(\mu)_i e^{-(\mu)_i z} / (\rho)_i (c_p)_i, & 0 \le r \le a, \\ 0\ , & a < r \le b \end{cases} \quad i = 1,2,3,4, \quad (35)$$

where the coefficients W_o, ρ, c_p and μ for the mask, gap, resist and substrate were chosen as listed in Table I. Here, we chose b= 5mm. For convenience, we take the exposed area to be circular (with radius $r = a$= 1mm) and in the center of the mask (Figure 2). However, it should be noted that in general, this area may not be in the center. Hence, it is necessary to consider a three-dimensional model. Furthermore, we chose a convection coefficient h_c = 0.006W/cm^2/K for the top of the mask. Without loss of generality, we considered a finite element mesh with the same 97 grid points in the xy-cross section, as shown in Figure 3, for each layer, and chose 50 grid points in the z-direction for mask, gap, resist and substrate, respectively. The time increment, Δt, was chosen to be 0.001. A linear basic function was chosen in each triangular element. The steady state solution was obtained when $\mathrm{Max}|(T^{n+1} - T^n)/T^{n+1}| \le 0.1$ per cent was satisfied in the resist.

Based on the above parameters, the steady state solution obtained on a SUN workstation gave a maximum temperature rise within the resist of 4.16K at the center when $n = 483$ with a CPU time of about 15 minutes. This maximum temperature rise is very close to 4.20K obtained by the preconditioned Richardson method (equation (34)) with $\omega = 1$. Figure 4 shows the transient temperature profiles along the central line in the z-direction. At the steady state case, there is good agreement with that obtained by the preconditioned Richardson method. Figure 5 shows contours of the steady state temperature distributions in the rz-cross section, which is similar to Figure 6 obtained using the preconditioned Richardson method. Since the silicon substrate thermal conductivity is three orders of magnitude greater than PMMA, the temperature

Properties	Beryllium (Weast, 1985)	He gas (100mbar) (Barron, 1985)	PMMA (Brandup and Immergut,1989)	Silicon (Weast, 1985)
k,W/cm/K	2.0	0.00152	0.00198	1.5
W,W/cm^2	2.042	0.0	1.823	1.424
μ, cm^{-1}	40.81	0.0	50.26	99.42
ρ, g/cm^3	1.85	0.000162	1.18	2.3
c_ρ, kJ/kg/K	0.436	5.2	1.42	0.715

Table I. Parameters used for the different layers

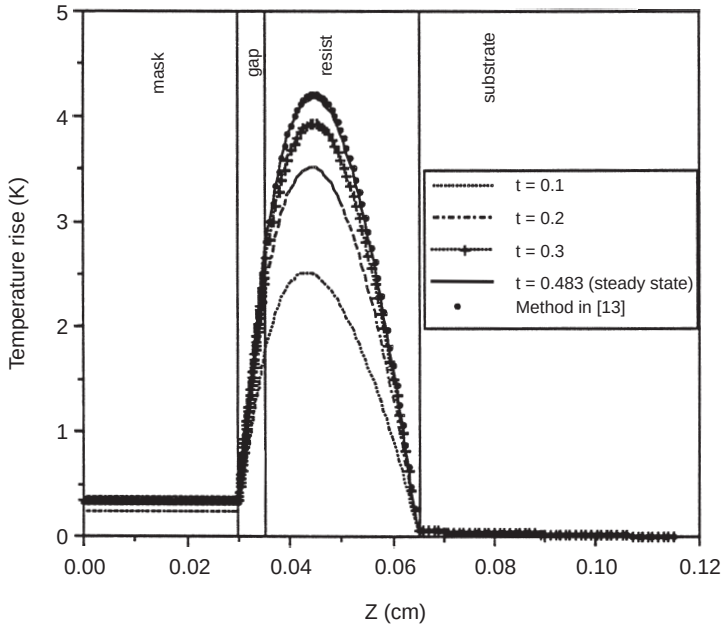

Figure 4.
Transient temperature profiles along the *z*-axis where the maximum temperature rise occurs in the resist

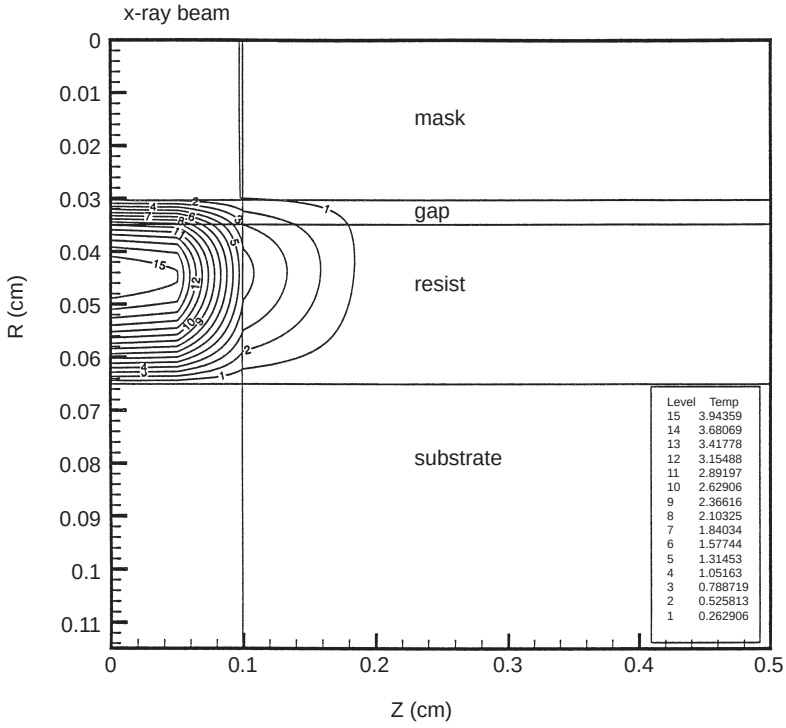

Figure 5.
Contours of the steady state temperature distribution in the *rz*-cross section

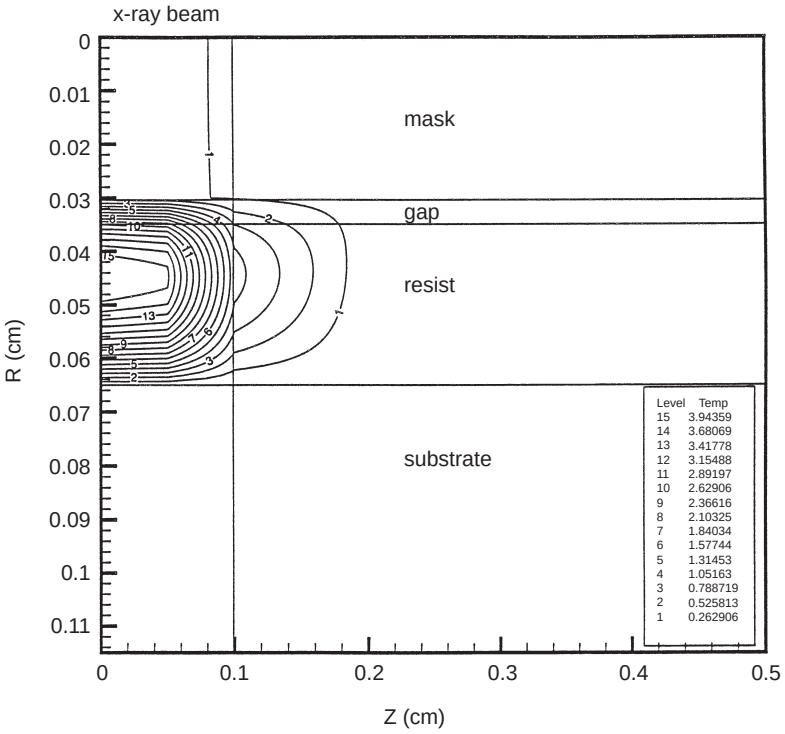

Figure 6.
Contours of the steady state temperature distribution in the *rz*-cross section obtained using the preconditioned Richardson method

distribution is nearly uniform over the substrate. From these figures, one can see that almost all of the heat added to the resist by the X-ray beam is transferred to the substrate rather than to the surrounding environment. This result is the same as that obtained in Ameel *et al.* (1994).

5. Conclusion

A three-dimensional numerical method for obtaining the temperature profile in an X-ray irradiation process is developed by using a hybrid finite element-finite difference scheme for solving three dimensional parabolic equations on thin layers with cylindrical geometry. A domain decomposition algorithm is then obtained based on a parallel Gaussian elimination for solving block tridiagonal linear systems. The method is illustrated by a numerical example. This method can be used for solving three dimensional parabolic equations on thin layers with arbitrary geometry in the *xy*-plane. Also, it can be applied in cases where surface scanning is used. An empirical experimental function was used to simulate heat source or energy deposition in the resist. However, the method is general where other source functions may be used. Further investigations are needed in order to determine how stress as influenced by temperature affects distortions in the mask and resist.

References

Ameel, T.A., Warrington, R.O., Yu, D. and Dahlbacka, G. (1994), "Thermal analysis of x-ray irradiated thick resists to determine induced structural deformations", *Heat Transfer*, Vol. 4, pp. 313-18.

Anton, H. (1994), *Elementary Linear Algebra*, 7th ed., Wiley, New York, NY.

Atkinson, K.E. (1988), *An Introduction to Numerical Analysis*, 2nd ed., John Wiley and Sons, New York, NY.

Barron, R. (1985), *Cryogenics Systems*, 2nd ed., Oxford University Press, New York, NY.

Brandup, J. and Immergut, E. (1989), *Polymer Handbook*, 3rd ed., John Wiley, New York, NY.

Canuto, C., Hussaini, M.Y., Quarteroni, A. and Zang, T.A. (1988), *Spectral Methods in Fluid Dynamics*, Springer-Verlag, New York, NY.

Carey, G.F. and Oden, J.T. (1984), *Finite Elements*, Vol. 3, Prentice-Hall, Englewood Cliffs, NJ.

Chandrupatla, T.R. and Belegundu, A.D. (1991), *Introduction to Finite Elements in Engineering*, Prentice-Hall, Englewood Cliffs, NJ.

Cole, K.D. and McGahan, W.A. (1993), "Theory of multilayers heated by laser absorption", *J. Heat Transfer*, Vol. 115, pp. 767-71.

Dai, W. and Nassar, R. (1997), "A three-dimensional numerical model for thermal analysis in x-ray irradiated photoresists with cylindrical domain", *Numerical Heat Transfer*, Part A, Vol. 32, pp. 517-30.

Dai, W. and Nassar, R. (1998a), "A three dimensional numerical method for thermal analysis in x-ray lithography", *Int. J. Numerical Methods for Heat & Fluid Flow*, Vol. 8, pp. 409-23.

Dai, W. and Nassar, R. (1998b), "A preconditioned Richardson numerical method for thermal analysis in x-ray lithography with cylindrical geometry", *Numerical Heat Transfer*, Part A, Vol. 34, pp. 599-616.

Dai, W., Nassar, R. Warrington, R.O. and Shen, B. (1997), "Three-dimensional numerical models for thermal analysis in x-ray irradiated photoresists", *Numerical Heat Transfer*, Part A, Vol. 31, pp. 585-95.

Feiertag, G., Ehrfeld, W., Lehr, H., Schmidt, A. and Schmidt, M. (1997), "Accuracy of structure transfer in deep X-ray lithograph", *Microelectronic Engineering*, Vol. 35, pp. 557-60.

Kant, R. (1988), "Laser-induced heating of a multilayered medium resting on a half-space: part I – stationary source", *J. Applied Mechanics*, Vol. 55, pp. 93-7.

Li, D.-C., Chen, J.-T., Chyuan, S.-W. and Sun, C.-Y. (1996), "Computer simulations for mask structure heating in X-ray lithography", *Computers & Structures*, Vol. 58, pp. 825-34.

Madison, M.R. and McDaniel, T.W. (1989), "Temperature distributions produced in an N-layer by static or scanning laser or electron beam with application to magneto-optical media", *J. Appl. Phys.* , Vol. 66, pp. 5738-48.

Manohara, H.M., Calderon, G., Klopf, J.M., Morris, K., Vladimirsky, O. and Vladimirsky, Y. (1996), "Temperature rise in thick PMMA resists during X-ray exposure", *Proc. of SPIE*, The International Society for Optical Engineering, Vol. 2880, pp. 183-90.

Ozisik, M.N. (1980), *Heat Conduction* , John Wiley and Sons, New York, NY.

Weast, R. (1985), *1985-86 CRC Handbook of Chemistry and Physics*, 66th ed., CRC Press, Boca Raton, FL.